Contact hyperfine field at Fe nuclei from density functional calculations

P. Novák*
Institute of Physics of ASCR, Cukrovarnická 10, 162 53 Prague 6, Czech Republic

V. Chlan
Faculty of Mathematics and Physics, Charles University, V Holešovičkách 2, 180 00 Praha 8, Czech Republic

(Received 10 December 2009; revised manuscript received 1 March 2010; published 17 May 2010)

The hyperfine field is an important probe of the magnetism of solids, yet its calculation from the first principles in the compounds of 3*d* metals proved to be difficult. For iron we circumvent this problem by calculating the spin magnetic moments of the 3*d* electrons and the valence 4*s* electrons and express the contact hyperfine field as their linear combination. After adding the contributions of the on-site interaction of the nuclear spin with the orbital and spin moment of the 3*d* electrons, the coefficients of the linear combination are calculated by comparison with the hyperfine field experimentally determined in a number of iron compounds. The method brings the theoretical contact fields within ~1 T of the values deduced from experiment.

DOI: 10.1103/PhysRevB.81.174412 PACS number(s): 76.60.−k, 71.15.Mb

I. INTRODUCTION

The density functional theory with local spin density approximation (LSDA) or semilocal [generalized gradient approximation (GGA)] approximations for the exchange-correlation potential proved to be immensely valuable for understanding of the magnetic properties of solids. Yet there exist several shortcomings of LSDA and GGA when applied to the magnetic systems. In the present paper we concentrate on one of them—severe underestimation of the contact hyperfine field B_c on the nuclei of 3*d* metal atoms.[1,2] Compared to B_c, the magnetic moments of these atoms are in much better agreement with the experiment. For the ^{57}Fe nuclei this circumstance is used in the present paper to obtain in a semiempirical way the correction to contact field calculated by the GGA.

In the past there were several attempts to calculate the contact hyperfine field on the Fe nuclei *ab initio*. In particular for bcc Fe Akai and Kotani[3] obtained very good agreement with the experiment using the optimized effective potential method. This method, however, is computationally very expensive and it was never used to calculate the hyperfine field in iron compounds. Novák *et al.*[2] obtained much improved values of B_c for bcc iron as well as for several iron compounds using computationally inexpensive, DFT based method proposed by Lundin and Eriksson.[4] It was recognized later, however, that Lundin and Eriksson functional violates important sum rule for the exchange-correlation hole, which is imposed by the density functional theory. This brings several shortcomings, e.g., incorrect energy of the core states and the functional is no longer in use.

Two papers most relevant to our present work are devoted to the hyperfine field on the Fe nuclei in metallic systems. Blügel *et al.*[5] studied the hyperfine field on the 3*d* and 4*d* impurities in nickel, while Ebert *et al.*[6] calculated the hyperfine fields of Ni and Fe in the Ni_xFe_{1-x} alloys. Their results are compared to ours in Sec. V.

The contact field originates from the nonzero electron spin density in a close vicinity of the nuclei,[5] and because of it, only the *s*-type electrons contribute to B_c. For the purpose of the analysis given below, we treat separately the contribution B_{val} of electrons in the valence *ns* orbitals ($n \geq 4$) and the contribution B_{core} of the core *s* orbitals (1*s*, 2*s*, and 3*s*),

$$B_c = B_{\mathrm{core}} + B_{\mathrm{val}}. \tag{1}$$

The core orbitals are fully occupied and corresponding spin density at the nucleus is connected with the different radial part of the wave function for spin-up and spin-down *ns* states. This difference is close to zero for a nonmagnetic atom in compounds or alloys with other magnetic atoms. For the 3*d* atoms and in most other cases it increases with increasing on-site electronic spin.[1,5,6] As the dominant part of the iron atomic spin is due to the unpaired 3*d* electrons and the occupation of the *ns* orbitals with $n \geq 5$ is very small, we can assume that

$$B_{\mathrm{core}} = B_{\mathrm{core}}(m_{3d}), \quad B_{\mathrm{val}} = B_{\mathrm{val}}(m_{3d}, m_{4s}), \tag{2}$$

where m_{3d}, m_{4s} are spin magnetic moments of the 3*d* and 4*s* electrons, respectively. B_{val} depends on both m_{3d}, m_{4s} as the nonzero density on the nucleus arises on one hand from difference of spin-up and spin-down 4*s* states population and, on the other hand, analogously as for the core states, from the difference of radial functions of these states. In principle the electrons in the *p* states polarize the *ns* electrons too. Our calculations showed that their magnetic moment is by more than two orders of magnitude smaller than m_{3d}, however, and the effect of the *p* states is not considered in what follows. For similar reasons the polarization of core states by the 4*s* electrons is also neglected.

It is often assumed that the functional dependences in Eq. (2) are linear[5,6] and the calculations presented in this paper confirm this assumption. The contact hyperfine field can be thus approximated as

$$B_c = a_{3d} m_{3d} + a_{4s} m_{4s}, \tag{3}$$

where a_{3d}, a_{4s} are parameters to be determined.

The hyperfine field B_{hf} may be written as the sum of the isotropic (i.e., independent of the direction of the spin) and anisotropic components

TABLE I. Compounds considered. In all compounds, but bcc Fe only the absolute value of B_{iso} was determined. The signs follow from the discussion in Sec. VI. FeF_3 is an antiferromagnet and the experimental value refers to total hyperfine field (see discussion in Sec. VI).

Compound	Symmetry	Fe site	Local symmetry	B_{iso} (T)	Ref.
$Y_3Fe_5O_{12}$	Cubic	Octahedral *a*	Trigonal	55.254	7
(YIG)		Tetrahedral *d*	Tetragonal	−47.348	
$Lu_3Fe_5O_{12}$	Cubic	Octahedral *a*	Trigonal	54.61	8
(LuIG)		Tetrahedral *d*	Tetragonal	−46.74	
$Li_{0.5}Fe_{2.5}O_4$	Cubic	Octahedral *B*	Rhombic	51.074	9
(Li ferrite)		Tetrahedral *A*	Trigonal	−51.936	
$MnFe_2O_4$	Cubic	Octahedral *B*	Trigonal	−51.074	10
(Mn ferrite)					
Fe_3O_4	Cubic	Octahedral *B*	Trigonal	−48.29	11 and 12
(magnetite)		Tetrahedral *A*	Cubic	50.77	
$BaFe_{12}O_{19}$	Hexagonal	Octahedral 2*a*	Trigonal	−54.68	13
		Bipyramidal 2*b*	Trigonal	−42.64	
		Tetrahedral $4f_4$	Trigonal	52.77	
		Octahedral $4f_6$	Trigonal	55.40	
		Octahedral 12*k*	Rhombic	−50.83	
FeF_3	Rhombohedral	Octahedral	Rhombic	−61.81	14
bcc Fe	Cubic	Octahedral	Cubic	−33.9	1

$$B_{hf} = B_{iso} + B_{aniz}. \tag{4}$$

The contact field is isotropic and in the compounds considered below it makes a dominating part of B_{iso}, though there are two other terms contributing:

$$B_{iso} = B_c + B_{orb}^{iso} + B_{dip}^{iso}, \tag{5}$$

where $B_{orb}^{iso}, B_{dip}^{iso}$ are isotropic parts of the magnetic dipolar interaction of the nuclear spin with the on-site electron orbital and spin magnetic moments.[5] Combination of Eqs. (3) and (5) gives

$$B_{iso} = a_{3d} m_{3d} + a_{4s} m_{4s} + B_{orb}^{iso} + B_{dip}^{iso}. \tag{6}$$

A number of experimental data on the isotropic component B_{iso} of the hyperfine field on the ^{57}Fe nuclei exist and we collect them in the next section. The *ab initio* calculation of the electronic structure yields both the magnetic moments m_{3d}, m_{4s} and the fields B_{orb}^{iso} and B_{dip}^{iso}. Using the experimental values of B_{iso} the parameters a_{3d}, a_{4s} may be then estimated.

II. COMPOUNDS CONSIDERED

Most of the compounds considered here possess either cubic or axial symmetry, the local symmetry of the Fe site is often lower, however (Table I). To extract B_{iso} from the experimental hyperfine field its anisotropic part B_{aniz} (i.e., dependence of the hyperfine field on the direction of the spin magnetic moment) must be separated first. This dependence reflects the local symmetry of the Fe site. In what follows, we assume that the spin magnetic moment is parallel to the magnetization. Neglecting terms of third and higher order, the hyperfine field B_{hf} may be written as

$$B_{hf} = B_{iso} + B_\vartheta(\vartheta_z^2 - 1/3) + B_\varepsilon(\vartheta_x^2 - \vartheta_y^2), \tag{7}$$

where $\vartheta_x, \vartheta_y, \vartheta_z$ are directional cosines of the magnetization referred to the local coordinate system of the site in question. If the local symmetry of the site is cubic, $B_{hf}=B_{iso}$. If the local symmetry is axial $B_\varepsilon=0$.

III. DETERMINATION OF $B_{orb}^{iso}, B_{dip}^{iso}$

The interaction of the nuclear spin with orbital moment of the electrons localized on the same site is nonzero only if the orbital moment is nonzero[5] and this in turn requires the presence of the spin-orbit coupling. The anisotropy of B_{orb} reflects the anisotropy of the orbital moment. In the compounds considered the ratio of anisotropic and isotropic parts of the Fe orbital moment is small and the same then holds for B_{orb}. The interaction between the nuclear and electron-spin moments has different character. The low-symmetry crystal field makes the electron-density nonspherical, and providing that the atom is magnetic, the dipolar interaction gives rise to the hyperfine field whether or not the spin-orbit coupling is present. If crystal field is strong compared to the spin-orbit coupling, the spatial distribution of electron density only slightly depends on the direction of magnetization and consequently the isotropic part of B_{dip} is small, in contrast to B_{orb}.

Analogously to B_{hf} [Eq. (7)], orbital moment, as well as B_{orb} and B_{dip} reflect the local symmetry of the 3*d* metal site. This can be used when determining the isotropic components of these quantities either from the calculation or from an experiment. We first define the center of the gravity of a quantity *X* as

$$X_{cg} = \sum_{i=1}^{N} n_i X(\vartheta_{ix}, \vartheta_{iy}, \vartheta_{iz}), \tag{8}$$

where the summation is over N crystallographically equivalent sites, n_i is the multiplicity of the site, and $X(\vartheta_{ix}, \vartheta_{iy}, \vartheta_{iz})$ is the value of quantity for given direction of the magnetization relative to the ith local coordinate system. X_{cg} complies with the crystal symmetry and, as a consequence, it is isotropic for the cubic systems, providing that the terms of order higher than two in direction cosines of the magnetic moment may be neglected. The isotropic part X^{iso} of the quantity in question is then

$$X^{\text{iso}} = X_{cg} / \sum_{i=1}^{N} n_i. \tag{9}$$

For systems with symmetry lower than cubic the situation is more complicated, as X_{cg}, beside the isotropic term, contains also terms quadratic in direction cosines of the magnetic moment. To determine the isotropic part of the quantity the calculation or measurement must be then carried out for two directions if the crystal symmetry is axial or for three directions in the case of rhombohedral symmetry.

We note that the orbital moment in the 3d metals is underestimated by as much as 50% when calculated using LDA or GGA (Ref. 1) and this should lead to similar underestimation of B_{orb} in bcc Fe. In iron compounds the situation is unclear. The experimental data on the orbital moment are controversial for the magnetite[15,16] and not available for other systems considered. On the computational side the GGA+U compared to GGA may either increase or decrease the orbital moment depending on the details of the energy band structure.

IV. DETAILS OF CALCULATION

The electronic structure was calculated with the full potential augmented plane waves+local orbitals (APW+lo) method, as implemented in the WIEN2k package.[17] The 1s, 2s, 2p, and 3s states of the 3d metal atoms were treated as the core states, while 3p, 3d, 4s, and 4p were included as the valence states. The sensitivity of the results to the parameters of the APW+lo was checked. For the exchange-correlation potential we adopted the GGA form.[18] The radii of the atomic spheres were 2 a.u. for Fe and Mn, 1.5 a.u. for the oxygen and the fluorine, 2.5 a.u for Ba, Lu, and Y, and 1.7 a.u. for Li.

The manganese ferrite $MnFe_2O_4$ was assumed to have normal spinel distribution of the cations, i.e., all octahedral (B) sites were occupied by iron, while tetrahedral (A) sublattice was filled with the manganese. The calculations for the magnetite were carried out in the cubic structure, which this compound possesses above the Verwey transition.

In all cases the experimental spin structure was assumed: ferromagnetic for bcc Fe, antiferromagnetic for FeF_3, and ferrimagnetic for the ferrites. The unit-cell parameters were taken from the literature, while the internal parameters for garnets, spinels, and the barium hexaferrite were obtained by optimization.

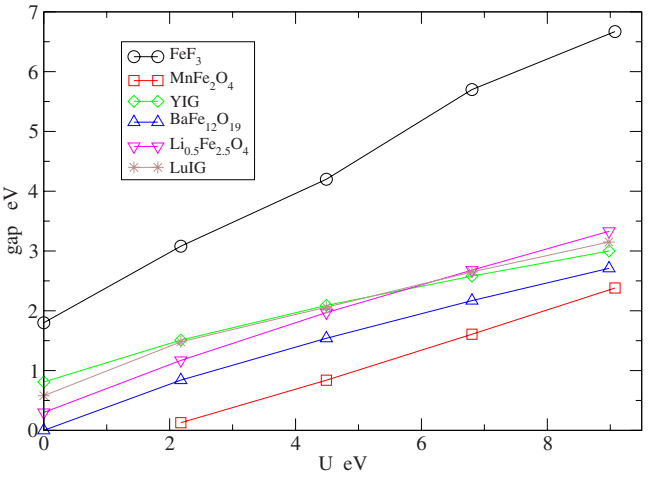

FIG. 1. (Color online) Dependence of the gap on parameter U.

The 3d electrons of the 3d metal ions in oxides and fluorides are strongly correlated and this correlation is not correctly described by either LSDA or GGA. As a consequence the gap is too small and in fact in two ferrites considered here there is no gap at all (Fig. 1). To improve the description of electron correlation we used the rotationally invariant version of the LDA+U method as described by Liechtenstein *et al.*[19] but with the GGA instead of LSDA exchange-correlation potential and only single parameter $U_{\text{eff}}=U-J$ (hereafter the subscript eff is dropped). The value of the parameter U=4.5 eV was adopted for Fe in oxides and FeF_3 for Mn in $MnFe_2O_4$ U=4 eV was chosen. The GGA+U method lowers the energy of the occupied states and increases the energy of the less occupied or empty states. As a consequence the gap E_g increases, its dependence on U being approximately linear (Fig. 1). In FeF_3, E_g is appreciably larger than in the oxide ferrites, reflecting more ionic state of the fluorides compared to the oxides.

In most of the oxides in question, as well as in FeF_3, the formal valency of iron is +3, the 3d shell is half filled and the application of GGA+U does not bring any problem. More complicated is the situation of iron on octahedral sites of Fe_3O_4. In this case the formal valence of the Fe(B) ions is +2.5, the system is half-metallic with Fe(t_{2g}), minority-spin bands, crossing the Fermi energy. If the magnetization is along a general direction and the spin-orbit coupling is included, there are four inequivalent Fe(B) ions in the unit cell. The GGA+U amplifies the inequivalency and leads to a charge disproportionation. To avoid this physically incorrect situation, we put the magnetization along the [001] direction. For $\vec{M} \| [001]$ all Fe(B) are equivalent and thus no disproportionation can occur.

The calculations of the gap did not include the spin-orbit coupling. Its effect on gaps is small and it would make the calculations time consuming. To find out the orbital moments and B_{orb}, B_{dip} we included the spin-orbit coupling using the second variational treatment.[20] By putting the magnetization along several different directions we checked that the angular dependence of the hyperfine field is well described by Eq. (7), i.e., fourth-order terms in direction cosines of the mag-

TABLE II. Results of the calculation. The hyperfine fields are in units of T, magnetic moments are expressed in μ_B. B_c^{calc} is the sum of the contribution of valence (B_{val}) and core (B_{core}) electrons.

Compound	Site	$B_{\text{orb}}^{\text{iso}}$	$B_{\text{dip}}^{\text{iso}}$	m_{3d}	m_{4s}	B_{val}	B_{core}	B_c^{calc}
$Y_3Fe_5O_{12}$	a	−0.672	0.003	−4.0919	−0.0108	−14.42	53.50	39.08
	d	0.747	−0.013	3.9367	0.0144	19.50	−50.67	−31.18
$Lu_3Fe_5O_{12}$	a	−0.495	0.003	−4.1045	−0.0107	−14.1	53.62	36.61
	d	0.613	−0.005	3.9462	0.0111	14.74	−51.70	−36.96
$Li_{0.5}Fe_{2.5}O_4$	B	0.623	−0.002	4.1047	0.0110	16.67	−53.61	−36.93
	A	−0.761	0.002	−3.9824	−0.0271	−14.63	51.70	37.07
$MnFe_2O_4$	B	0.418	0.235	4.1167	0.0153	20.55	−53.61	−33.06
Fe_3O_4	B	5.188	−3.721	3.8265	0.0118	15.94	−50.15	−34.22
	A	−0.928	−0.048	−3.9414	−0.0100	−13.34	51.17	37.83
$BaFe_{12}O_{19}$	$2a$	0.518	−0.001	4.1049	0.0117	15.59	−53.39	−37.80
	$2b$	0.720	0.029	3.9832	0.0175	23.50	−51.50	−27.99
	$4f_4$	−0.774	−0.001	−3.9710	−0.0102	−13.59	51.51	37.93
	$4f_6$	−0.579	0.000	−4.0658	−0.0095	−12.82	52.98	40.16
	$12k$	0.576	0.003	4.0924	0.0149	20.02	−53.13	−33.11
FeF_3		0.310	−0.005	4.2765	0.0090	11.61	−56.13	−44.52
bcc Fe		2.378	−0.175	2.346	−0.0033	−4.49	−28.59	−32.75

netization may be neglected. The results of GGA+U calculations with the spin-orbit coupling included are collected in Table II.

V. VALENCE AND CORE CONTRIBUTIONS TO CONTACT FIELD

There is hardly a way to separate experimentally the contribution of the valence and core electrons to the hyperfine field, even more difficult would be to find out the dependence of B_c on the valence and core spin. On the other hand to obtain this information using the electron structure calculation is relatively straightforward. In Fig. 2 the dependence of the valence contribution B_{val} on the spin moment of Fe $4s$ electrons is displayed. As seen in Fig. 2 the valence part of B_c is to a very good approximation linear function of m_{4s}. Close correlation between B_{val} and m_{4s} was also found by Ebert *et al.*[6] for both Fe and Ni in Ni_xFe_{1-x} alloys.

The dependence of the core contribution B_{core} to the contact field on the spin moment of the $3d$ electrons is shown in Fig. 3. The situation is more complex here comparing to B_{val}. The dependence is again approximately linear, but there are only few data for m_{3d} smaller than $3.9\mu_B$ and the dispersion of the data is bigger. As showed in Ref. 6 the linear proportionality between B_{core} and the local Fe moment holds $B_{\text{core}}=a_{\text{Fe}}\mu_{\text{Fe}}$ in Ni_xFe_{1-x} alloys with $a_{\text{Fe}}=-10.4\mu_B/\text{T}$. Similar value $a_{\text{Fe}}=-10.6\mu_B/\text{T}$ was obtained by Blügel *et al.* for the Fe impurity in Ni. These values are not far from the value $a_{3d}=-12.19\ \text{T}/\mu_B$ calculated using the data for bcc Fe in Table II. The linear fit to the data for all compounds considered (dashed line in the inset of Fig. 3) gives slightly higher value $a_{3d}=-12.8\mu_B/\text{T}$.

Inspection of Figs. 2 and 3 reveals that magnitude of B_{val} is smaller than that of B_{core}, though contribution of B_{val} to the contact field is significant.[7–10]

VI. ANALYSIS

There are several remarks to be made in connection with the B_{iso} values collected in Table I. In most cases only the absolute value of the hyperfine field was found experimentally. When attaching the sign to these values, we assumed that (i) the contact field is the dominating part of B_{hf} in the cases considered and (ii) though the calculations underestimate the B_c value, the underestimation is of order of few tens of %, so the signs of experimental B_{iso} and calculated B_c should coincide. Second remark concerns Fe_3O_4. The value of B_{iso} in Table I refers to the cubic structure that exists

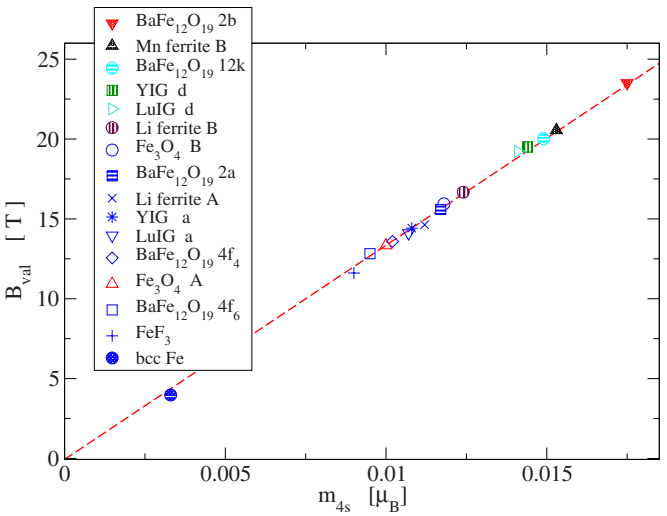

FIG. 2. (Color online) Dependence of the valence electrons contribution to the contact field on the $4s$ spin moment. The dashed line is a linear fit to the results: $B_{\text{val}}\cong a_{4s}m_{4s}$ with $a_{4s}=1339\ \text{T}/\mu_B$. To increase the resolution of the figure the sign of the data for bcc Fe was inverted.

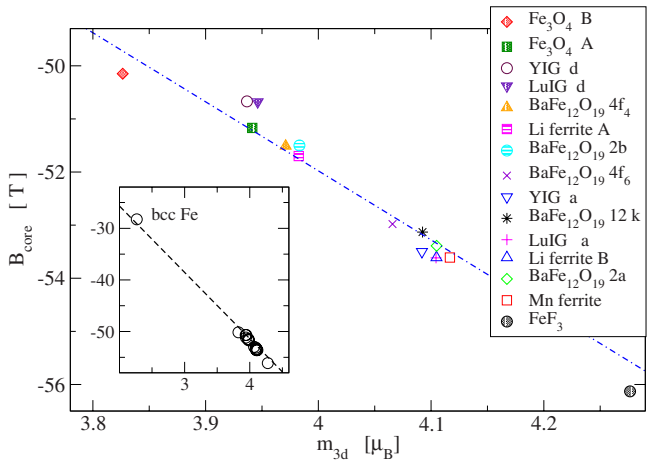

FIG. 3. (Color online) Dependence of the core $(1s,2s,3s)$ contribution to B_c on the spin moment of $3d$ electrons. The inset shows all compounds considered, dashed line is corresponding linear fit to the data. In the main body of the figure the interval $m_{3d}>3.8\mu_B$ is enlarged, dash and dotted line is linear fit to the data, excluding bcc Fe.

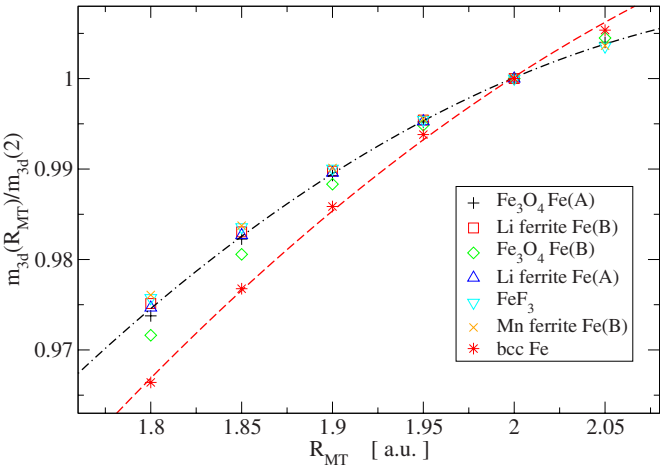

FIG. 4. (Color online) Dependence of the ratio of $3d$ electron-spin moment $m_{3d}/m_{3d}(R_{MT}=2$ a.u.) on the radius of atomic sphere. Dashed (dashed and dotted) curve serves as a guide for eyes only.

above the Verwey temperature $T_V\cong 122$ K, while the calculations correspond to the absolute zero temperature. Using the experimental data in Refs. 11 and 12 the extrapolation of $B_{\rm iso}(T\geq T_V)$ to the zero temperature presents little problem, however. Final problem concerns FeF_3. This compound is antiferromagnetic,[13] only the total value of $B_{\rm hf}$ was determined experimentally[14] and to our knowledge there is no information on the direction of magnetic moments. For FeF_3 it is thus not possible to determine experimental value of $B_{\rm iso}$. The GGA+U calculation showed, however, that the anisotropy of $B_{\rm orb}$, $B_{\rm dip}$ is negligible (less than 0.001 T) and the classical dipolar field from the spin moments on the other sites of the lattice is rather small $B_{\rm hf}^{\rm lattice}\sim -0.03$ T. To a good approximation we may therefore assume that in this case $B_{\rm iso}\cong B_{\rm hf}$

From the results obtained it follows that m_{3d} and m_{4s} are two quantities that should be treated as independent. In the next section we fit the experimental $B_{\rm iso}$ assuming that the dependences in Eq. (2) are linear, though the parameters may differ from the dependences calculated *ab initio*. We note that except for FeF_3 the $B_{\rm hf}^{\rm lattice}$ is not needed, as it does not possess the isotropic part.

VII. DISCUSSION

There are several stumbling blocks in the analysis given above. First, in the density functional theory the magnetic spin moments of $3d$ or $4s$ electrons are not well defined quantities, even more important is that in the APW+lo method m_{3d} and m_{4s} depend on the radius of the atomic sphere R_{MT}. To see how serious is this dependence, $m_{3d}(R_{MT})$ is displayed in Fig. 4, while m_{4s} as a function of R_{MT} is shown in Fig. 5. It is seen that $3d$ moments depend only slightly on the R_{MT}, while for the $4s$ moments the dependence is an order of magnitude stronger. The strongest effect has the radius of atomic sphere for bcc Fe, for which the decrease in R_{MT} from 2 to 1.8 a.u. reduces m_{4s} by $\sim 75\%$.

The second serious problem is that our calculations depend on the parameter U (bcc Fe being an exception as $U=0$ was used in this case). The increase in U makes the majority spin $3d$ electrons more localized. As a consequence the $3d$ spin magnetic moment increases monotonically (Fig. 6) and its value saturates for large U, reaching $5\mu_B$ for compounds where nominal valency of iron is 3+. The dependence of the $4s$ spin magnetic moment on U is displayed in Fig. 7. For both $3d$ and $4s$ electrons the dependence is smooth although the data for different compounds span larger interval comparing to their dependence on the atomic sphere radius and the fits showed in Figs. 6 and 7 serve as a guide for eyes only.

The last point to be discussed is the dependence of $B_{\rm orb}^{\rm iso}$ on the parameter U. As mentioned in Sec. III, $B_{\rm orb}$ is proportional to the orbital moment. For Fe^{3+} the orbital moment appears thanks to the not fully occupied (fully empty) majority (minority) $3d$ spin states. As U is increased, energy of the

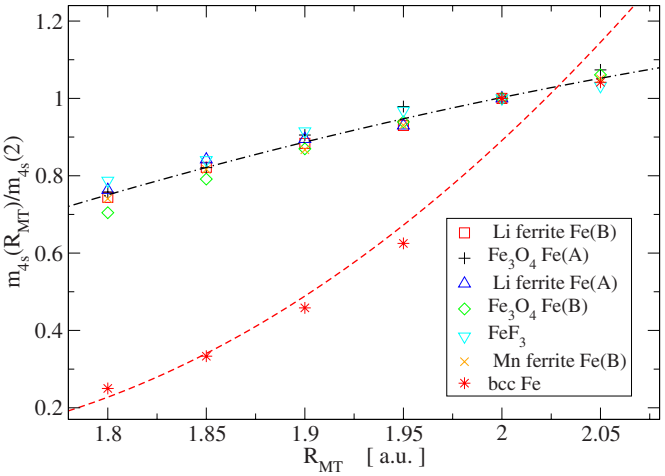

FIG. 5. (Color online) The same as Fig. 4, but for the $4s$ valence electrons.

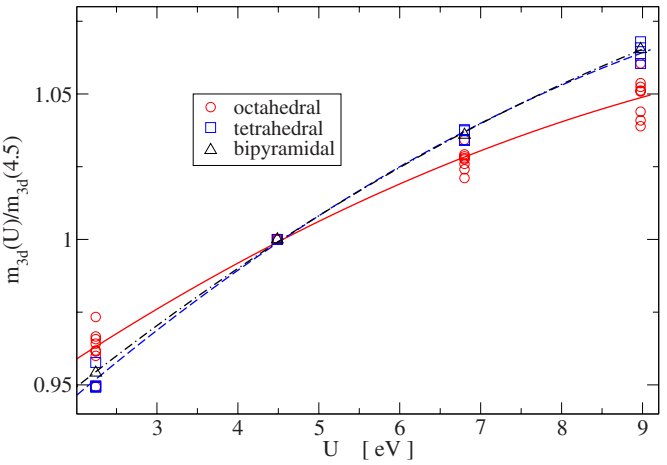

FIG. 6. (Color online) Dependence of the ratio of $3d$ magnetic moments $m_{3d}(U)/m_{3d}(U=4.5\ \text{eV})$ on the parameter U. The curves correspond to a quadratic fit to data for tetrahedral (dashed), octahedral (full), and bipyramidal (dashed and dotted) coordination.

majority spin states is lowered and their occupation increases, the opposite holds for the minority-spin states. As a consequence the orbital moment and B_{orb} decrease. The calculation for FeF_3, $MnFe_2O_4$, and tetrahedral Fe in magnetite showed that the dependence is approximately linear, magnitude of $B_{\text{orb}}^{\text{iso}}$ decreases by ~50% as U is changed from 2 to 9 eV. Inspection of Table II shows that corresponding uncertainty in $B_{\text{orb}}^{\text{iso}}$ is smaller than 0.5 T. Interestingly, for iron on the octahedral site of magnetite, for which the formal valency is 2.5, $B_{\text{orb}}^{\text{iso}}$ is almost independent of U in this interval.

The comparison between values of B_{iso} obtained from the experiment, values calculated using Eq. (6) and those determined by WIEN2k is given in Table III. It is seen that comparing to WIEN2k the analysis of the preceding section qualitatively improves the agreement with the experiment, reducing the mean deviation $\delta=|\langle B_{\text{iso}}^{\text{exp}}-B_{\text{iso}}^{\text{calc}}\rangle|$ from 15.7 to 1.3 T. The parameters in Eq. (6) have values $a_{3d}=-15.86\ \text{T}/\mu_B$, $a_{4s}=959.6\ \text{T}/\mu_B$.

Despite the improvement there remains a serious discrepancy for bcc Fe. In this case, because the $3d$ electrons are

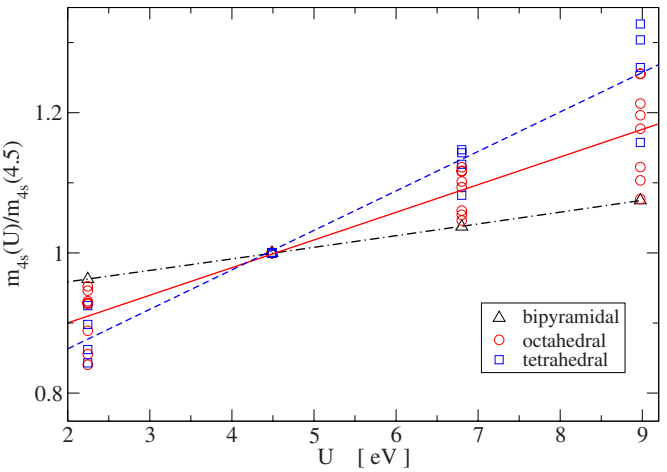

FIG. 7. (Color online) Analogous to Fig. 6, but for the $4s$ valence electrons and the fits of the data are linear.

TABLE III. Comparison of the isotropic parts of the hyperfine field. The values $B_{\text{iso}}^{\text{exp}}$ deduced from the experiments are confronted with $B_{\text{iso}}^{\text{calc}}$ calculated using Eq. (6) with the parameters a_{3d} and a_{4s} determined using the data for all compounds. $B_{\text{iso}}^{(1)\text{calc}}$ were determined excluding the data bcc Fe. $B_{\text{iso}}^{\text{WIEN2k}}$ refer to isotropic parts of the hyperfine field as calculated by the WIEN2k program.

Compound, site	$B_{\text{iso}}^{\text{exp}}$	$B_{\text{iso}}^{\text{calc}}$	$B_{\text{iso}}^{(1)\text{calc}}$	$B_{\text{iso}}^{\text{WIEN2k}}$
bcc Fe	−33.90	−37.99		−30.65
YIG a	55.25	53.86	54.52	38.41
YIG d	−47.35	−47.88	−47.15	−30.44
LuIG a	54.61	54.34	55.04	39.03
LuIG d	−46.74	−48.45	−47.82	−30.87
Li-ferrite B	−51.07	−52.48	−52.56	−36.19
Li-ferrite A	51.94	51.90	52.37	36.22
Mn-ferrite B	−51.07	−49.96	−49.10	−32.41
$BaFe_{12}O_{19}$ $2a$	−54.68	−53.36	−53.72	−37.28
$2b$	−42.64	−45.63	−43.89	−27.25
$4f_4$	52.77	52.42	53.14	37.15
$4f_6$	55.40	54.79	55.85	39.58
$12k$	−50.83	−50.03	−49.29	−32.53
FeF_3	−61.81	−58.88	−60.34	−44.22
Fe_3O_4 A	50.77	51.94	52.70	33.46
B	−48.29	−47.90	−47.93	−32.04
bcc Fe	−33.90	−37.00		−30.65

much more delocalized than in the rest of the compounds considered, we used GGA and not GGA+U. Imperfect treatment of the electron correlations could then cause the discrepancy.

Because of the above uncertainty of GGA calculation for bcc Fe the coefficients a_{3d} and a_{4s} were determined excluding bcc Fe. The results are denoted as $B_{\text{iso}}^{(1)\text{calc}}$ in Table III and it is seen that calculated B_{iso} is in a fair agreement with $B_{\text{iso}}^{\text{exp}}$, the mean deviation δ being smaller than 1 T. The expansion coefficients in units of T/μ_B are

$$a_{3d}=-16.92, \quad a_{4s}=1229. \tag{10}$$

It is of interest to compare these values with the values obtained by fitting the data calculated using WIEN2k (Figs. 2 and 3): $a_{3d}^{\text{WIEN2k}}=-12.99$, $a_{4s}^{\text{WIEN2k}}=1339\ \text{T}/\mu_B$. Clearly GGA based calculation underestimate the contribution of the core $1s$, $2s$, and $3s$ electron, while giving correctly the valence part of the B_c once bcc Fe is excluded from the fitting procedure. This is in line with the good agreement between measured and calculated hyperfine field in special cases when B_c is dominated by the transferred hyperfine interaction (as for Cu impurities in Fe, Co, and Ni,[5,21,22] where B_c originates mainly from the spin polarization of Cu $4s$ valence states via interactions with the magnetic neighbors).

Inspection of Table III reveals that to obtain parameters [Eq. (10)] mostly the compounds containing nominally trivalent iron were used, iron on the B site of the magnetite being the only exception. Because Fe^{3+} is an S-state ion the orbital moment and consequently also $B_{\text{orb}}^{\text{iso}}$ is rather small. Although

qualitatively orbital moment is given correctly by the GGA (GGA+U) calculation, its numerical value often differs from the value deduced from the experiment.[1] As the contact hyperfine field depends only on the spin moments and not on the valency, the values [Eq. (10)] should be reliable.

VIII. CONCLUSIONS

We believe that Eq. (6) in conjunction with the parameters given by Eq. (10) provide a suitable tool to explain and predict the values of the contact field on the Fe nuclei in iron compounds containing ferric ions in the high spin d^5 electron configuration, where the orbital moment is small. These systems include ferrites with spinel and garnet structure, W-, Y-, and M-hexaferrites, maghemite, hematite, hydrated ferrites, and possibly others. We also believe that the results can be useful even when orbital moment of Fe is bigger. In these cases the method can provide relatively reliable contact field. Comparison with the experiment could then shed more light on the discrepancy of local and semilocal approximations to DFT when calculating the orbital moment dependent quantities.

When calculating the electronic structure, we treated the iron in different environments in as homogeneous way as possible, in particular the radius of Fe atomic sphere R_{MT} =2 a.u. and the parameter U=4.5 eV in the GGA+U method were used. This seemingly limits applicability of the method. We note, however, that the dependence of the magnetic moments on these parameters is smooth (Figs. 4–6) and the interpolation in case that other values of these parameters are used does not represent problem.

ACKNOWLEDGMENTS

This work was supported by the Grant Agency of the Academy of Sciences of Czech Republic under Project No. IAA100100803 and by the project KONTAKT ME08059.

*novakp@fzu.cz

[1] R. Coehoorn, J. Magn. Magn. Mater. **159**, 55 (1996).
[2] P. Novák, J. Kuneš, W. E. Pickett, W. Ku, and F. R. Wagner, Phys. Rev. B **67**, 140403(R) (2003).
[3] H. Akai and T. Kotani, Hyperfine Interact. **120-121**, 3 (1999).
[4] U. Lundin and O. Eriksson, Int. J. Quantum Chem. **81**, 247 (2001).
[5] S. Blügel, H. Akai, R. Zeller, and P. H. Dederichs, Phys. Rev. B **35**, 3271 (1987).
[6] H. Ebert, H. Winter, B. L. Gyorffy, D. D. Johnson, and F. J. Pinski, J. Phys. F: Met. Phys. **18**, 719 (1988).
[7] P. Novák, J. Englich, H. Štěpánková, J. Kohout, H. Lütgemeier, K. Wagner, and W. Tolksdorf, Phys. Rev. Lett. **75**, 545 (1995).
[8] V. Chlan, P. Novák, H. Štěpánková, J. Englich, J. Kuriplach, and D. Nižňanský, J. Appl. Phys. **99**, 08M903 (2006).
[9] V. D. Doroshev, V. A. Klochan, N. M. Kovtun, and V. N. Seleznev, Phys. Status Solidi A **9**, 679 (1972).
[10] H. Štěpánková, B. Sedlák, V. Chlan, P. Novák, and Z. Šimša, Phys. Rev. B **77**, 092416 (2008).
[11] P. Novák, H. Štěpánková, J. Englich, J. Kohout, and V. A. M. Brabers, Phys. Rev. B **61**, 1256 (2000).
[12] Proceedings of the ICF8, Kyoto, Tokyo, Japan, 2000, edited by M. Abe and Y. Yamazaki (The Japan Society of Powder and Powder Metallurgy, Tokyo, 2000).
[13] H. Štěpánková, J. Englich, E. G. Caspary, and H. Lütgemeier, J. Magn. Magn. Mater. **177-181**, 253 (1998).
[14] G. K. Wertheim, H. J. Guggenheim, and D. N. E. Buchanan, Phys. Rev. **169**, 465 (1968).
[15] D. J. Huang, H. J. Lin, and C. T. Chen, Phys. Rev. Lett. **96**, 039702 (2006).
[16] E. Goering, M. Lafkioti, and S. Gold, Phys. Rev. Lett. **96**, 039701 (2006).
[17] P. Blaha, K. Schwarz, G. K. H. Madsen, D. Kvasnicka, and J. Luitz, in *WIEN2k, An Augmented Plane Wave+Local Orbitals Program for Calculating Crystal Properties*, edited by K.-H. Schwarz (Technische Universtät, Wien, Austria, 2001).
[18] J. P. Perdew, K. Burke, and M. Ernzerhof, Phys. Rev. Lett. **77**, 3865 (1996).
[19] A. I. Liechtenstein, V. I. Anisimov, and J. Zaanen, Phys. Rev. B **52**, R5467 (1995).
[20] D. J. Singh, *Plane Waves, Pseudopotentials, and the LAPW Method* (Kluwer Academic, Dordrecht, 1994).
[21] P. H. Dederichs, R. Zeller, H. Akai, and H. Ebert, J. Magn. Magn. Mater. **100**, 241 (1991).
[22] V. S. Stepanyuk, R. Zeller, P. H. Dederichs, and I. Mertig, Phys. Rev. B **49**, 5157 (1994).